NASA-TM-79311 19800005977

NASA Technical Memorandum 79311

CORROSION RESISTANCE OF SODIUM SULFATE COATED COBALT-CHROMIUM-ALUMINUM ALLOYS AT 900°, 1000°, AND 1100° C

G. J. Santoro
Lewis Research Center
Cleveland, Ohio

November 1979

SUMMARY

A series of cobalt-rich alloys in the cobalt-chromium-aluminum system were coated once with 1 mg/cm^2 of Na_2SO_4 and exposed at temperatures of 900°, 1000°, and 1100° C for 100-one hour cycles. The extent of the corrosion was measured and the results compared to the cyclic oxidation of alloys with the same composition and to the hot corrosion of compositionally equivalent nickel-base alloys. Cobalt alloys with sufficient aluminum content to form aluminum containing scales corroded less than their nickel-base counterparts. The cobalt alloys with lower aluminum levels formed CoO scales and corroded more than their nickel-base counterparts which formed NiO scales.

INTRODUCTION

Alloys in the nickel(Ni)-rich - chromium(Cr)-aluminum(Al) system and the cobalt(Co)-rich - Cr-Al system are being used for high-temperature applications such as coatings or as the basis for high-strength gas turbine alloys. Recently in this laboratory cyclic oxidation (ref. 1) and hot corrosion (ref. 2) studies were performed on alloy compositions in these two ternary systems. In the Ni-base ternary system, compositions possessing good cyclic oxidation resistance were found to also possess good cyclic hot corrosion resistance.

Alloys in the cobalt ternary system were found to be less cyclic oxidation resistant than their compositionally equivalent Ni-base alloys under the severe conditions of long time exposure to high temperatures (1100°-1200° C). Under these severe conditions the base element oxides replaced the more protective αAl_2O_3-aluminate spinels. The CoO formation led to massive spalling while NiO failed in a more gradual and predictable manner.

The objective of this paper was to evaluate the hot corrosion resistance of Co-rich - Cr-Al alloys and compare the results with those from the previously tested Ni-base alloys of the same Cr and Al compositions. This comparison was intended to determine the effect of the cobalt matrix vs. the nickel matrix on the corrosion of alloys from these two systems. Coupon specimens of nine compositions were coated once with 1 mg/cm^2 of Na_2SO_4 and cyclic heated in furnaces at ambient atmosphere to temperatures of 900°, 1000°, and 1100° C. The extent of the corrosion was evaluated by measuring the maximum depth of attack into the specimen, the weight change and the amount of spallation. The results were compared to those obtained from the hot corrosion results of the compositionally equivalent Ni-base alloys.

MATERIALS

All of the alloys prepared in this program were vacuum melted in zirconia crucibles and cast in zirconia shell molds as is common in commercial practice. Trace zirconium pickup of up to 0.5 wt.% was detected in all the alloys in this series. Each mold consisted of a "tree" of ten 2.5×5.1×0.25 cm coupons, each

with its own riser. For each coupon used, the riser was removed and analyzed for Cr and Al by atomic absorption. Table I gives the compositions of the Co-Cr-Al alloys used in this investigation and the comparable Ni-Cr-Al alloys evaluated in reference 2. Also listed are the average Cr and Al compositions of the equivalent Ni- and Co-base alloys. These average compositions were used as input in the regression analysis described later. After casting the coupons were cut and ground into 1.3×2.3×0.23 cm pieces. All samples then had a hanger hole drilled at one end and were glass bead blasted. After ultrasonic cleaning, the samples were ready for testing.

PROCEDURE

Test Procedures

Prior to testing sample dimensions were measured and in particular the thickness was measured to a precision of ±1 μm. Prior to insertion into the furnace, samples were coated with 1 mg/cm^2 of reagent grade Na_2SO_4. Application of the salt coating was accomplished by heating a weighed sample on a hot plate set at about 200° C and spraying one side with a saturated solution of Na_2SO_4 using an airbrush. The sample was then cooled and weighed to check for the correct amount of salt deposited. The same procedure was used to coat the other side of the specimen. The samples were then ready for testing in cyclic furnaces which have been described in detail in reference 3. One such furnace is shown schematically in figure 1. Samples were thermally cycled to allow 1 hour at temperature and a minimum of 40 minutes cooling in static air. Samples reached the highest test temperature in less than two minutes after insertion into the furnace and cooled to ambient temperature in less than 20 minutes after removal from the furnace. Samples of each alloy were exposed for 100 cycles at 900°, 1000°, and 1100° C. Weight change was determined at regular intervals throughout the test. At the conclusion of the furnace testing the accumulated spall for each sample was weighed and examined by X-ray diffraction. Each corroded sample was also examined by X-ray diffraction and by metallography. The thickness of the remaining alloy visibly unaffected by the corrosion attack was measured on metallographically prepared cross-sections with a microscope cathetometer at a magnification of ×100. The original thickness minus the above measurement with the difference divided by two is defined here as the maximum depth of penetration of the corrosion attack.

Regression Analysis

A digital computer program, NEWRAP (ref. 4), was used to perform a regression analysis on the data. The purpose of this analysis was to express the corrosion in terms of alloy composition and to compare the corrosion of the Co-base alloys to their compositionally equivalent Ni-base alloys so as to evaluate matrix element effect on corrosion. A two independent variable 2nd order polynomial model was apriori judged suitable for this data. The dependent vari-

able was the maximum depth of corrosion, D, and the two independent variables were C and A, the atom percent concentrations of chromium and aluminum, respectively, in the alloy. The concentration values came from table I. These values were the averages for the equivalent nickel- and cobalt-base alloys. Since the maximum depth of attack, D, may be expected to have the same relative error over a wide range of values, the dependent variable was transformed into the logarithm of D. The process is termed homogenizing the error variance. To evaluate the matrix element effect on corrosion the dummy variable approach was used (ref. 5). This was accomplished by adding to the terms of the 2nd order polynomial equation described above an identical set of terms each multiplied by a dummy variable, Z. The variable Z was set to one to represent the cobalt-base alloys and to zero to represent the nickel-base alloys. Thus the model equation used was:

$$\log D = B_0 + B_1C + B_2A + B_3C^2 + B_4A^2 + B_5CA$$

$$B_6 1/T + ZB_7 + ZB_8C + ZB_9A + ZB_{10}C^2 + ZB_{11}A^2 + ZB_{12}CA + ZB_{13}1/T$$

where the Bs are the coefficients whose values and significance must be determined; T is the absolute temperature and the other terms have already been identified. Nonsignificant terms were deleted from the model equation by the back-rejection technique (ref. 5), where the critical significance level was supplied as input. A significance level of 90 percent was chosen here. In this method if the coefficients of all the terms containing a dummy variable were to be deleted as insignificant then this result would be interpreted as meaning the effect of the matrix element, cobalt or nickel, was insignificant in the corrosion process under the conditions of this test, that is, a cobalt and a nickel alloy with the same Cr and Al content would corrode to the same extent. On the other hand if all or some of the coefficients of terms containing the dummy variable were found to be significant, then their sign and magnitude would determine whether the cobalt or equivalent nickel alloy corroded more.

RESULTS

Measure of Corrosion

The extent of corrosion was measured by the net specific weight change, the accumulated weight of spall and the maximum depth of attack. These data are presented in table II. In general the three measures of corrosion gave consistent results. Samples which changed little in weight usually spalled only slightly and had relatively little depth of attack. In most cases the weight of spall collected was the same as the weight that was lost indicating spallation was a prominent factor in the alloys' degradation. Figures 2(a) to (c) contain the kinetic data for the corrosion at 900°, 1000°, and 1100° C, respectively. The data from most of

the alloys can be represented by a relatively narrow band of weight changes vs. time. But alloys 12 and 17 are well out of this band. As will be shown in the next section the morphology of these two alloys differs markedly from those of the other alloys.

X-ray Diffraction and Metallography

After the furnace exposure both the retained and the spalled oxides were identified by X-ray diffraction (XRD). The oxide phases detected by XRD are listed in table III. Figures 3(a) to (c) is a graphical presentation the XRD analysis of the retained scales only. Various sodium, sulfur, and oxygen compounds were detected along with the metal oxide phases. For simplicity the sodium containing phases were not listed in table III or figure 3. A definite relationship is observed in the changes occurring in the oxide phases with temperature via the XRD data. Thus an alloy that forms mostly Al_2O_3 or spinel at 900° C will form more CoO at 1100° C. The less the aluminum content in the alloy to begin with the more pronounced is this effect as there is less of a reservior of aluminum to replace that which is lost by the corrosion process. This observation correlates with the data in table II where the amount of spalling increases with temperature. Thus as the temperature increases the formation of CoO increases as does the extent of spallation.

The loss of aluminum from near the surface of those alloys on which aluminum containing oxides are predominantly formed during corrosion is also reflected by the presence of depleted zones beneath the oxide scale as seen in the photomicrographs of cross-sections of specimens corroded at 1100° C (figs. 4(a) to (i)). The photo micrographs of specimens exposed at 1100° C are presented here as their morphologies are more readily discernable than those at lower temperatures, although the features are essentially the same. Alloys 12 and 17, figures 4(c) and (h) possess a distinctively different morphology from the other alloys. Instead of a thin retained scale over a depleted zone with internal corrosion particles, there exists a thick double layered scale. The outer scale is dense and columnar while the inner scale is porous. The outer scale was identified by XRD as predominantly CoO. The thickness of the outer scale prevented a positive identification of the phases within the inner scale. This scale structure has been observed to occur often in oxidation of cobalt-chromium alloys (ref. 6). Since CoO is less protective than any of the other oxide phases observed here, a different kinetic behavior would be expected for alloys 12 and 17. This difference in kinetic behavior is observed in figure 2. The β phase in alloys 12 and 17 (figs. 4(a) and (h)), are aligned perpendicular to the surface. This configuration is present throughout the entire cross-section and resulted from the fabrication of these specimens and not the corrosion process.

The distribution of the elements near the surface of corroded specimens is presented in figure 5 and in figure 6. Figure 5 represents those alloys with a thin retained scale over a depleted zone and figure 6 the double layered scale. In the former both the retained scale and the internal corrosion particles were rich in

aluminum and low in cobalt. The matrix of the depleted zone was low in aluminum compared to the substrate. At longer times at temperature it would be expected that there would be insufficient aluminum to supply a protective aluminum containing scale. The sulfur distribution was difficult to determine but appears to be concentrated in an area just beneath the depleted zone.

The double layered structure in figure 6 was rich in cobalt, as expected, and was also rich in chromium, particularly within the inner porous scale. The aluminum seems concentrated at the scale - substrate interface together with the sulfur.

Regression Results

At 900° and 1000° C the differences in the extent of corrosion among the alloys were not sufficient to obtain a clear understanding of the relationship of corrosion to the aluminum and chromium contents or to ascertain a possible matrix effect. At 1100° C the model equation reduced to the following significant terms:

$$\log D = 3.55450 - 0.121045C - 2.61032\times10^{-2}A + 4.20087\times10^{-3}C + 0.11953ZC$$

$$- 7.74191\times10^{-2}ZA - 7.06125\times10^{-3}ZC^2 + 3.95417\times10^{-3}ZCA \pm 8.91114\times10^{-2}$$

Since the coefficients of some of the terms containing the dummy variable, Z, are significant, a matrix effect does exist. The complexity of the equation prevents a readily discernible identification of the matrix effect and of the variation of the corrosion with concentration. A graphical representation of the equation is presented in figure 7. The corrosion isopleths of both the nickel and cobalt-base alloys are shown. The average composition used for the computer input of the alloys tested is also shown. For simplicity the identification numbers are for the cobalt-base alloys only but the equivalent nickel-base alloy identifications are given in table IV. In figure 7 the hash lines mark areas where the corrosion of the two families of alloys overlap. Thus the cobalt alloys 10 and 15 corroded to the same extent as the nickel alloys 1 and 9. The same is true of the cobalt alloys 12 and 17 and the nickel alloys 3 and 7. From figure 7 it would seem that cobalt-base alloys are more corrosion resistant than their compositionally equivalent nickel-base alloys when the concentrations of chromium and aluminum in the alloys are relatively high, about 18 at. % chromium and about 22 at. % aluminum. At lower compositions it would seem the two families of alloys corrode to the same extent. In both alloy systems the corrosion resistance increases with increase aluminum provided the chromium level is from about 10 to 20 at. %.

With greater resolution of the contours in figure 7, however, it would be seen that except for alloys 12 and 17, the cobalt-base compositions are more corrosion resistant than their equivalent nickel-base alloys, while alloys 12 and 17 are less resistant than their equivalent nickel-base alloys, 3 and 7, respectively. This relationship is evident in table IV. It should be recalled that the cobalt alloys 12 and 17 formed the double layered scale while all the other cobalt alloys formed predominantly aluminum containing scales. Also from reference 2, the predomi-

nant oxide formed on nickel alloys 3 and 7 was NiO, while the predominant retained scale of all the other equivalent nickel-base alloys was either Al_2O_3, Cr_2O_3 or spinel. Based on these data the matrix effect is difficult to interpret and will be discussed in some detail in the next section.

DISCUSSION

The interpretation of these results require some care. In these experiments the alloys were coated with Na_2SO_4 just the one time, at the beginning of the cyclic furnace exposure. And it is known that in many materials the hot corrosion mechanism is not self-sustaining but requires repetitive exposure to the condensed salt (e.g., see ref. 7). Without this repetitive exposure accelerated attack could decrease to a rate equivalent to that which the material would have in straight oxidation. As noted in the previous section the morphology of the retained scales on alloys 12 and 17 resembled those normally associated with straight oxidation, that is, a double layered scale, the outer scale dense and columnar and the inner scale porous. Thus it appears the corrosion mechanism was not self-sustaining and that the initial hot corrosion attack ceased and further corrosion proceeded essentially by straight oxidation. That hot corrosion occurred initially can be assumed since the total attack far exceeded that which occurred when these two alloys were cyclic oxidized at 1100° C without a Na_2SO_4 coating (table V). In straight cyclic oxidation the NiCrAls corroded less than the CoCrAls when the predominant oxide in the scale was that of the matrix element (ref. 1). Thus when alloys 12 and 17 approached the oxidation only stage, they corroded at a greater rate than their equivalent nickel-base alloys. As the tests were conducted here it is not known whether alloys 12 and 17 would have been more corrosion resistant than their nickel-base counterparts had the corrosion process been sustained by repetitive coatings of Na_2SO_4 on both systems.

Goebel and Pettit (ref. 7), have compared the hot corrosion of nickel and cobalt alloys containing about 25 weight percent chromium and about 6 weight percent aluminum. They concluded that although the mechanism of attack were essentially the same for both alloys, a combination of basic fluxing and preferential oxidation, the cobalt-base alloy was much more resistant to the initiation of hot corrosion attack than the nickel-base alloy during cyclic furnace testing with continual deposition of Na_2SO_4. The attack on these alloys was found not to be self-sustaining. If the composition of the alloys just discussed were plotted in figure 7, it would be predicted that the CoCrAl alloy would be much superior in resisting attack than the NiCrAl alloy, in agreement with their reported relative corrosion behavior. This agreement suggests that despite the lack of sustaining the hot corrosion attack with additional Na_2SO_4 deposits the results obtained here rightly reflects the comparative hot corrosion resistance of those alloys with sufficient aluminum and chromium to form Al_2O_3/spinel scales.

CONCLUDING REMARKS

The results found here can then be summarized as follows: In a nonsustained Na_2SO_4-induced hot corrosion attack, where the availability of condensed salt is limited, CoCrAl alloys possess superior corrosion resistance than their equivalent nickel-base alloys provided the scales formed are Al_2O_3/spinel. For those MCrAl alloys where the aluminum content is sufficiently low so that the scales consists of the oxide of the matrix element, the nickel-base alloys are superior to the cobalt-base alloys. Thus the cobalt matrix would seem to have conferred superior corrosion to those alloys with higher aluminum content, but the lack of a sustained attack precludes extending this conclusion to those alloys with less aluminum.

It can be expected that for very long durations at high temperatures even the alloys with higher Cr and Al concentrations will eventually become depleted of these elements to the point where the predominant oxide will be that of the matrix element. Since neither NiO and CoO scales offer sufficient protection for materials used as high temperature coatings, the corrosion life of the MCrAl alloys can be defined as being limited by the rate of Cr and Al depletion from the alloy.

REFERENCES

1. Barrett, C. A.; and Lowell, C. E.: The Cyclic Oxidation Resistance of Cobalt-Chromium-Aluminum Alloys at 1100° and 1200° C and a Comparison with the Nickel-Chromium-Aluminum Alloy System. Oxid. Met., vol. 12, no. 4, Aug. 1978, pp. 293-311.

2. Santoro, G. J.; and Barrett, C. A.: Hot Corrosion Resistance of Nickel-Chromium-Aluminum Alloys. J. Electrochem. Soc., vol. 125, no. 2, Feb. 1978, pp. 271-278.

3. Barrett, C. A.; and Lowell, C. E.: Comparison of Isothermal and Cyclic Oxidation Behavior of Twenty-Five Commerical Sheet Alloys at 1150° C. Oxid. Met., vol. 9, no. 4, Aug. 1975, pp. 307-355.

4. Sidik, S. M.: An Improved Multiple Linear Regression and Data Analysis Computer Program Package. NASA TN D-6770, 1972.

5. Draper, N. R.; and Smith, H.: Applied Regression Analysis. John Wiley & Sons, Inc., 1966.

6. Kofstad, P. K.; and Hed, A. Z.: Oxidation of Co-10w/oCr Interrupted by Vacuum Annealing. Oxid. Met., vol. 2, no. 1, May 1970, pp. 101-117.

7. Goebel, J. A.; and Pettit, F. S.: Hot Corrosion of Cobalt-Base Alloys. PWA-5379, Pratt & Whitney Aircraft, 1975. (ARL-TR-75-0235, AD-A024425.)

TABLE I. - CHEMICAL ANALYSIS OF AS-CAST MATERIALS[a]

Alloy	Matrix	Composition, at. %			
		Analyzed		Averaged for computer input	
		Chromium	Aluminum	Chromium	Aluminum
10	Co	15.86	18.30	15.9	17.9
1	Ni	15.98	17.54		
11	Co	11.55	20.97	12.0	21.8
2B	Ni	12.44	22.72		
12	Co	12.85	12.05	13.0	12.1
3	Ni	13.19	12.07		
13	Co	18.78	11.59	18.6	11.3
4	Ni	18.41	11.06		
14	Co	18.93	23.25	19.0	23.7
6B	Ni	19.19	24.24		
15	Co	10.46	18.25	10.1	17.7
9	Ni	9.73	17.18		
16	Co	13.07	24.55	13.7	24.1
5A	Ni	14.35	23.65		
17	Co	15.90	5.41	15.9	5.6
7	Ni	15.81	5.77		
18	Co	22.11	16.95	21.5	16.7
8B	Ni	20.84	16.52		

[a]All alloys melted in ZrO_2 crucibles with trace Zr pickup of up to 0.5 w/o Zr.

TABLE II. - CYCLIC CORROSION OF CoCrAl ALLOYS

[Specimens coated with 1 mg/cm^2 of sodium sulfate (Na_2SO_4); 100 hours at temperature.]

Alloy	Temperature, °C	Maximum depth of attack, μm	Specific weight change, mg/cm^2	Specific weight of accumulated spall, mg/cm^2
10	900	0	-0.66	0
	1000	28	-3.37	1.8
	1100	93	-9.46	8.4
11	900	20	-0.33	0.1
	1000	24	-3.34	2.6
	1100	88	-15.05	16.6
12	900	11	0.47	2.0
	1000	80	-17.66	9.6
	1100	346	-232.84	273.7
13	900	2	-0.08	0.2
	1000	65	-2.55	3.8
	1100	159	-25.80	33.0
14	900	0	-0.59	0.1
	1000	10	-1.86	0.9
	1100	60	-6.22	4.5
15	900	7	-0.03	0.1
	1000	28	.92	.3
	1100	109	-16.18	20.2
16	900	1	-0.56	0.1
	1000	14	-1.82	1.1
	1100	66	-12.05	10.9
17	900	85	-8.71	18.2
	1000	156	-9.29	28.3
	1100	324	-59.92	101.2
18	900	2	0.09	0
	1000	23	-2.03	1.1
	1100	79	-7.55	5.3

TABLE III. - OXIDE PHASES ON CORRODED SPECIMENS

Alloy	Temperature, °C	Oxide phases	
		Retained scale	Spalled scale
10	900	Al_2O_3	----------
	1000	Spinel, CoO	Al_2O_3, spinel, CoO
	1100	Spinel, Al_2O_3, Cr_2O_3	CoO, spinel, Al_2O_3
11	900	Al_2O_3	----------
	1000	Spinel, CoO	Al_2O_3, spinel, CoO
	1100	Spinel, CoO, Al_2O_3, Cr_2O_3	CoO, spinel, Al_2O_3
12	900	Spinel	CoO, spinel
	1000	CoO, spinel	CoO, spinel
	1100	CoO, spinel	CoO, spinel
13	900	Spinel, Al_2O_3	Spinel, CoO
	1000	Spinel, CoO	CoO, spinel
	1100	CoO, spinel, Cr_2O_3	CoO, spinel, Al_2O_3 (?)
14	900	Al_2O_3	Spinel
	1000	Spinel, Al_2O_3, Cr_2O_3	Al_2O_3, spinel, CoO
	1100	Spinel, Cr_2O_3, Al_2O_3, CoO	CoO, spinel, Al_2O_3, Cr_2O_3
15	900	Spinel, Al_2O_3	CoO, Cr_2O_3 (?)
	1000	Spinel, Al_2O_3	CoO, spinel, Cr_2O_3
	1100	Spinel, Cr_2O_3 (?)	CoO, Al_2O_3, spinel
16	900	Al_2O_3	----------
	1000	Spinel, Al_2O_3	Al_2O_3, spinel, CoO
	1100	Spinel, Al_2O_3	CoO, spinel, Al_2O_3
17	900	Spinel	Spinel, CoO
	1000	CoO, spinel	CoO, spinel
	1100	CoO	CoO, spinel
18	900	Al_2O_3, Cr_2O_3 (?)	----------
	1000	Spinel, Al_2O_3, Cr_2O_3	CoO, spinel, Al_2O_3, Cr_2O_3
	1100	Spinel, CoO, Al_2O_3, Cr_2O_3	CoO, spinel, Al_2O_3, Cr_2O_3

TABLE IV. - MAXIMUM DEPTH OF CORROSION

ATTACK AT 1100° C, 100 CYCLES

Alloy	Matrix	Maximum depth of attack, μm		
		Measured values	Average	Computer estimate
10	Co	95, 93, 92	93	116
1	Ni	136, 140, 142	139	162
11	Co	88, 88, 86	88	78
2B	Ni	168, 174, 163	168	134
12	Co	345, 352, 342	346	256
3	Ni	298, 219, 244	254	230
13	Co	169, 152, 156	159	151
4	Ni	363, 365, 359	362	277
14	Co	57, 64, 60	60	63
6B	Ni	176, 154, 160	163	136
15	Co	138, 97, 92	109	129
9	Ni	212, 192, 157	187	194
16	Co	72, 65, 60	66	62
5A	Ni	88, 87, 80	85	110
17	Co	279, 378, 314	324	366
7	Ni	238, 291, 344	291	333
18	Co	80, 79, 78	79	74
8B	Ni	244, 230, 218	231	273

TABLE V. - COMPARISON OF CORROSION WITH A Na_2SO_4 AND WITHOUT A Na_2SO_4 COATING AT 1100° C AND 100 CYCLES

Alloy	Weight change, mg/cm^2	
	Without Na_2SO_4[a]	With Na_2SO_4
12	-163	-233
17	+4	-60

[a]Calculated from the oxidation constants given in reference 1.

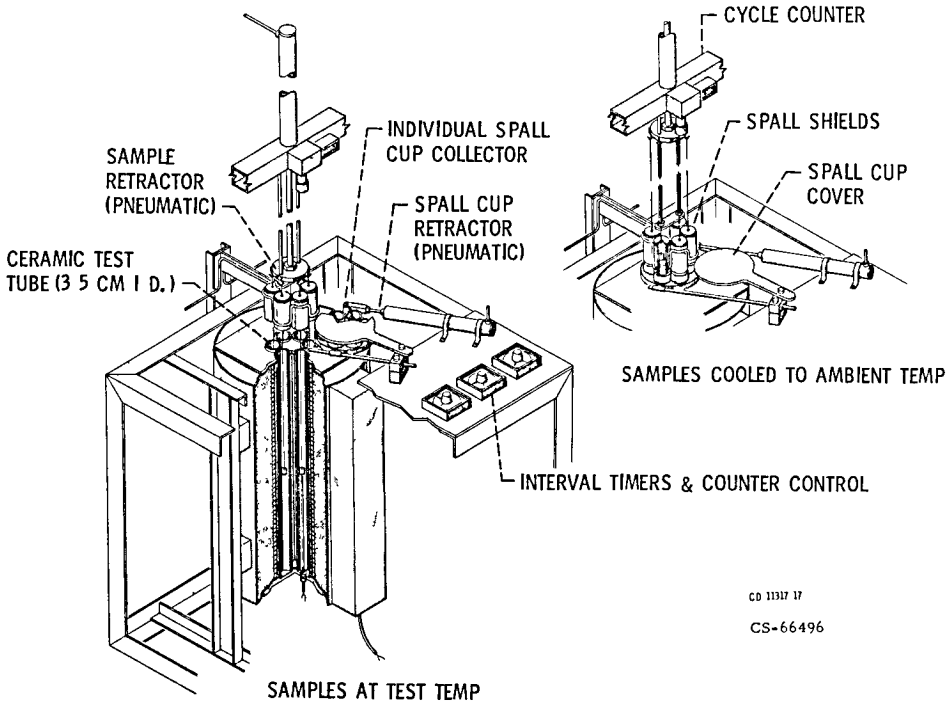

Figure 1 - Multitube automatic high temperature cyclic corrosion test rig

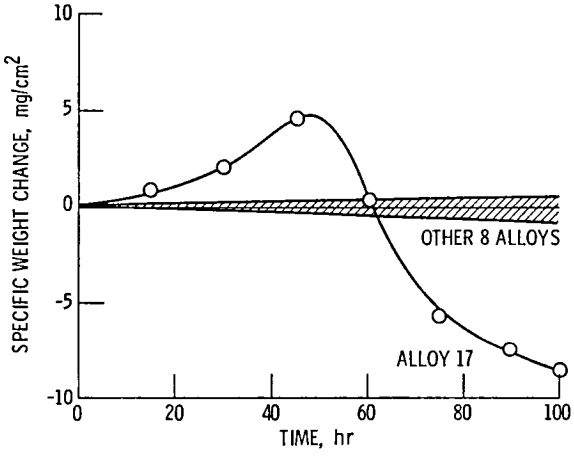

(a) CORROSION TEMPERATURE, 900° C

Figure 2 - Specific weight as function of time for Na_2SO_4 - coated CoCrAl alloys corroded at various temperature

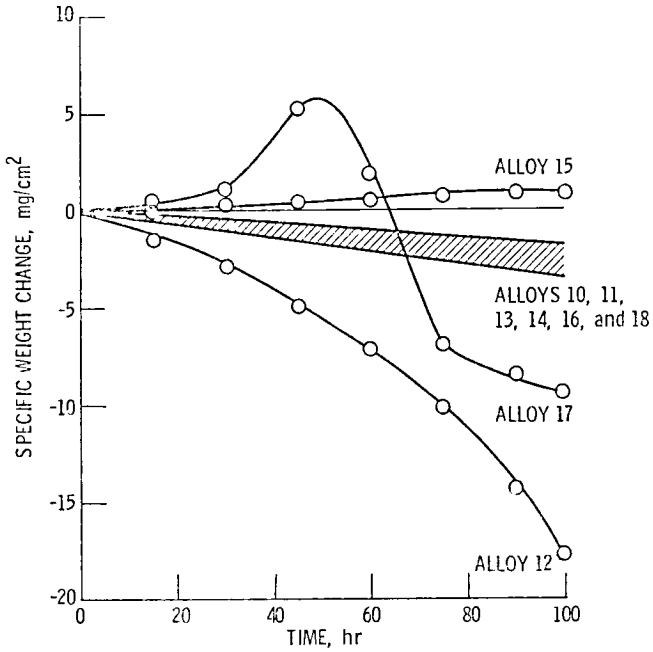

(b) CORROSION TEMPERATURE, 1000° C

Figure 2 - Continued

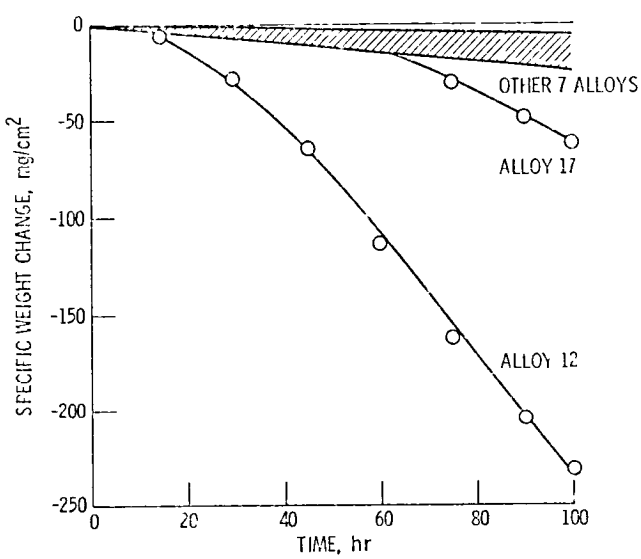

(c) CORROSION TEMPERATURE, 1100° C

Figure 2 - Concluded

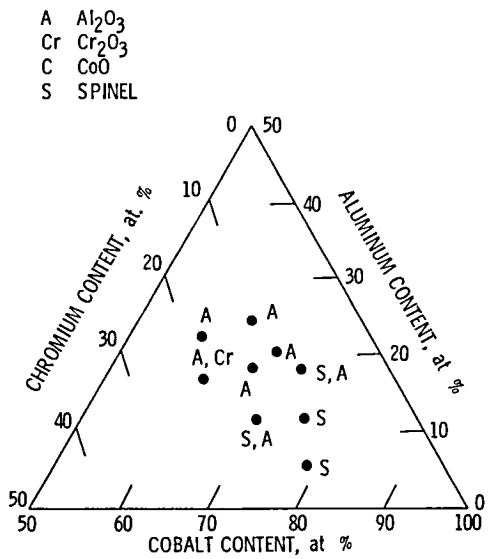

(a) CORROSION TEMPERATURE, 900° C

Figure 3 - Oxide phases in the retained scale of specimens corroded at various temperatures Phases listed in order of decreasing line intensities

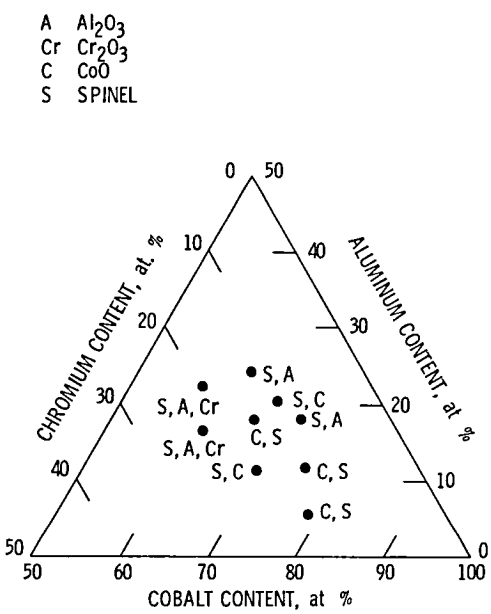

(b) CORROSION TEMPERATURE, 1000° C

Figure 3 - Continued

A Al_2O_3
Cr Cr_2O_3
C CoO
S SPINEL
(?) INSUFFICIENT LINES FOR POSITIVE IDENTIFICATION

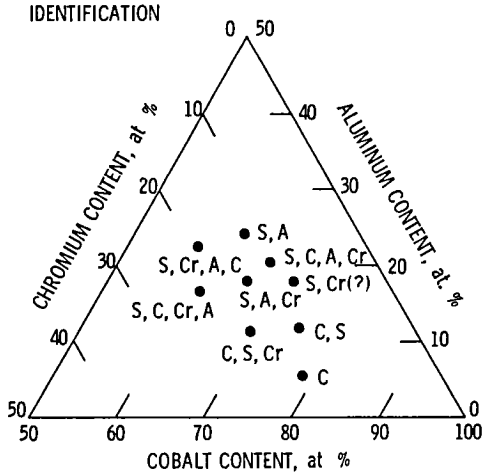

(c) CORROSION TEMPERATURE, 1100° C

Figure 3. - Concluded.

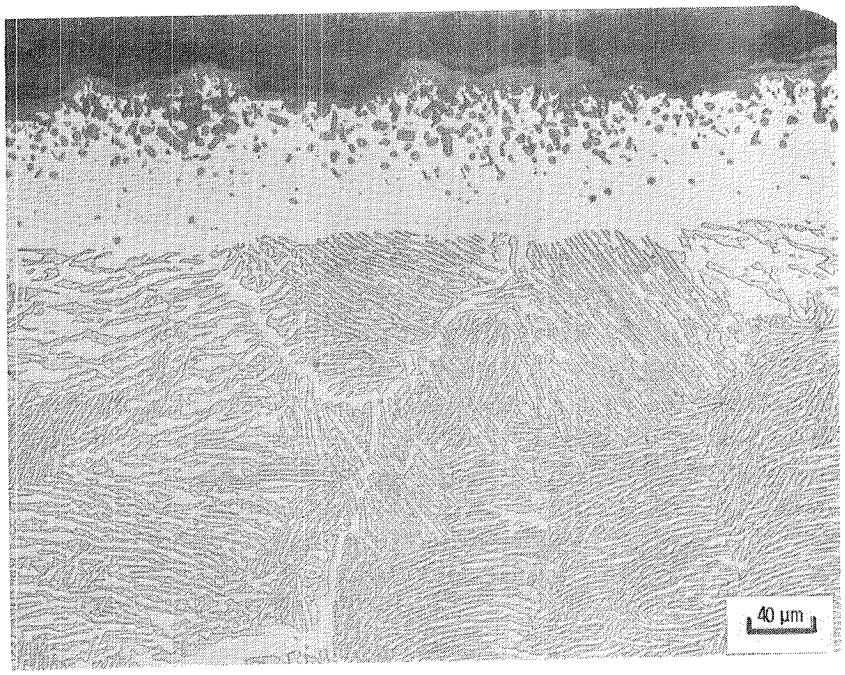

(a) Alloy 10, Co-15.86Cr-18.30Al.

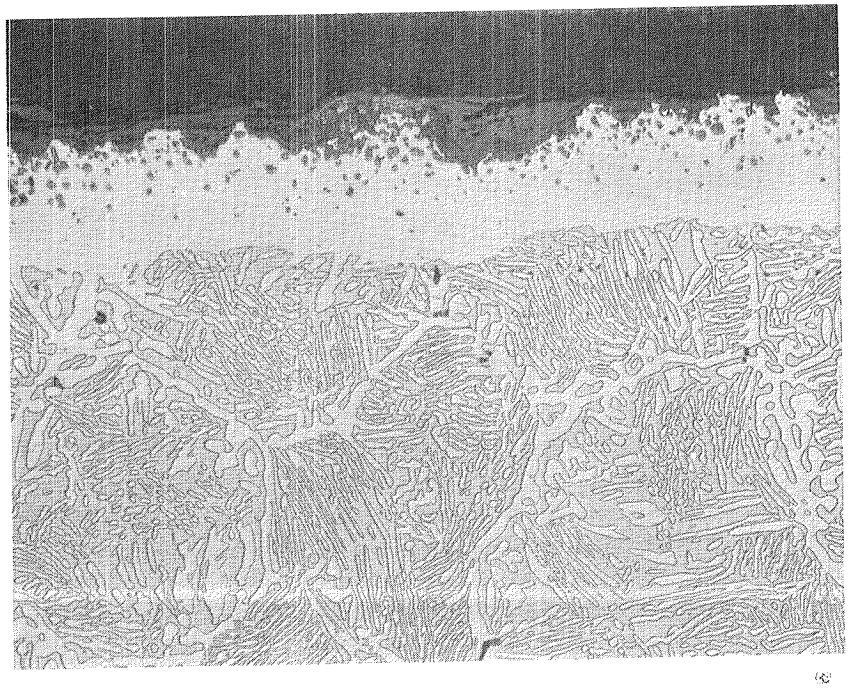

(b) Alloy 11, Co-11.55Cr-20.97Al.

Figure 4. - Microstructures of CoCrAl alloys after Na_2SO_4-induced hot corrosion at 1100° C and 100 cycles (1 hr at temperature - 40 min cooling). Compositions given as atom percent.

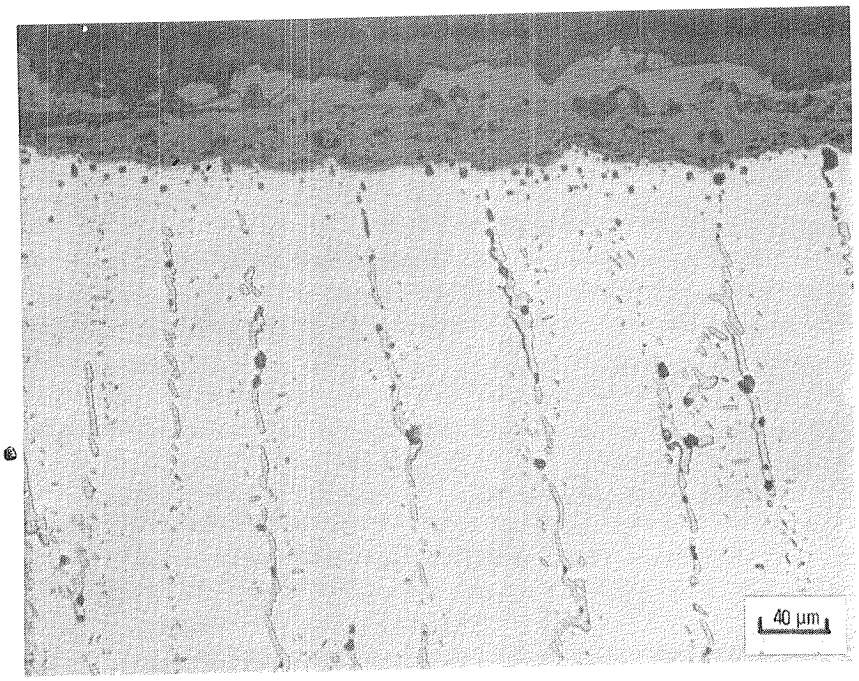

(c) Alloy 12, Co-12.85Cr-12.05Al.

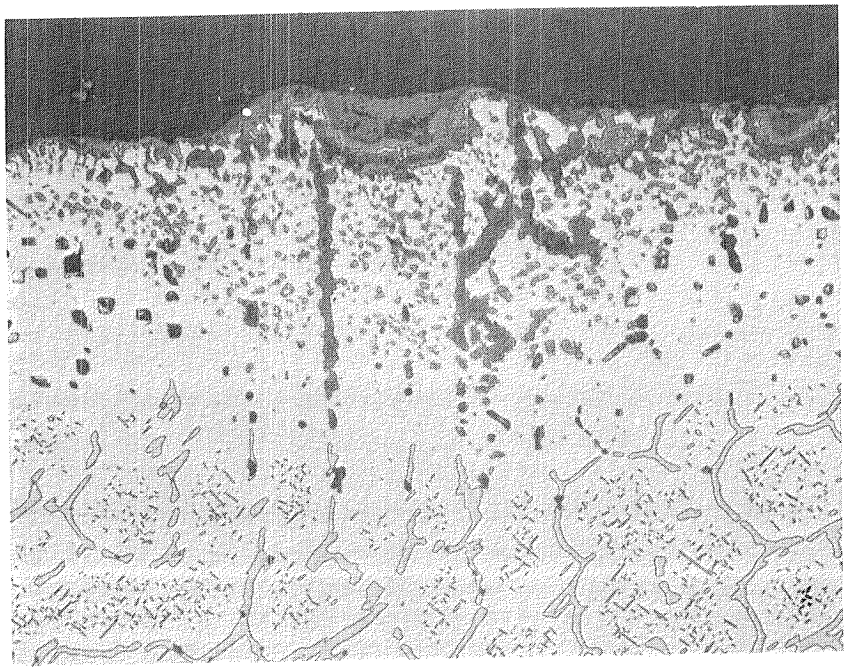

(d) Alloy 13, Co-18.78Cr-11.59Al.

Figure 4. - Continued.

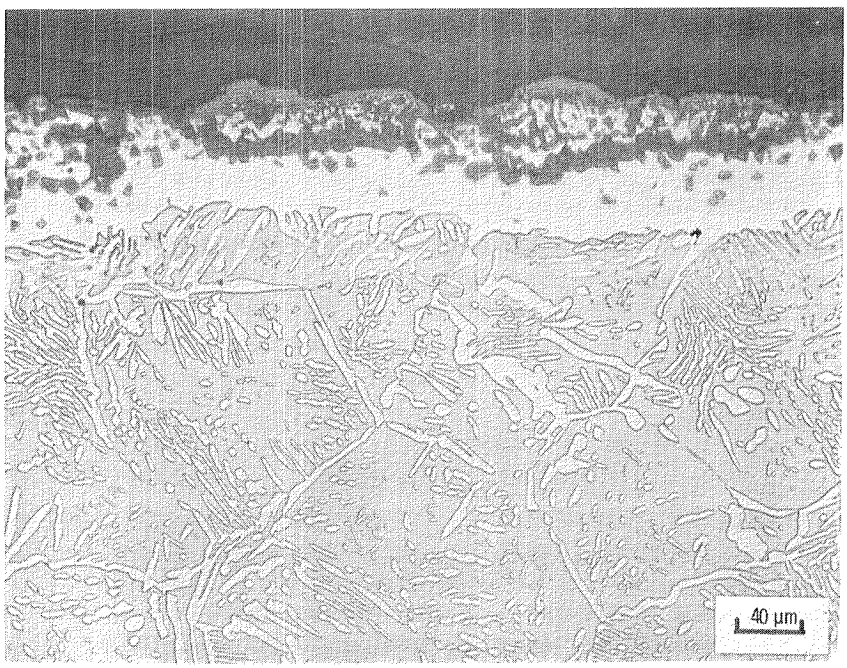

(e) Alloy 14, Co-18.93Cr-23.25Al.

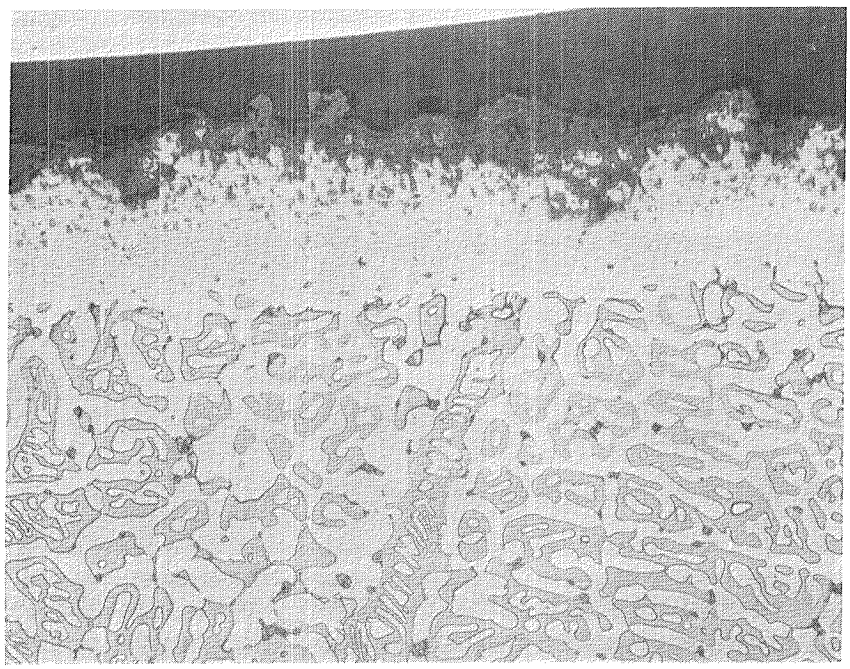

(f) Alloy 15, Co-10.46Cr-18.25Al.

Figure 4. - Continued.

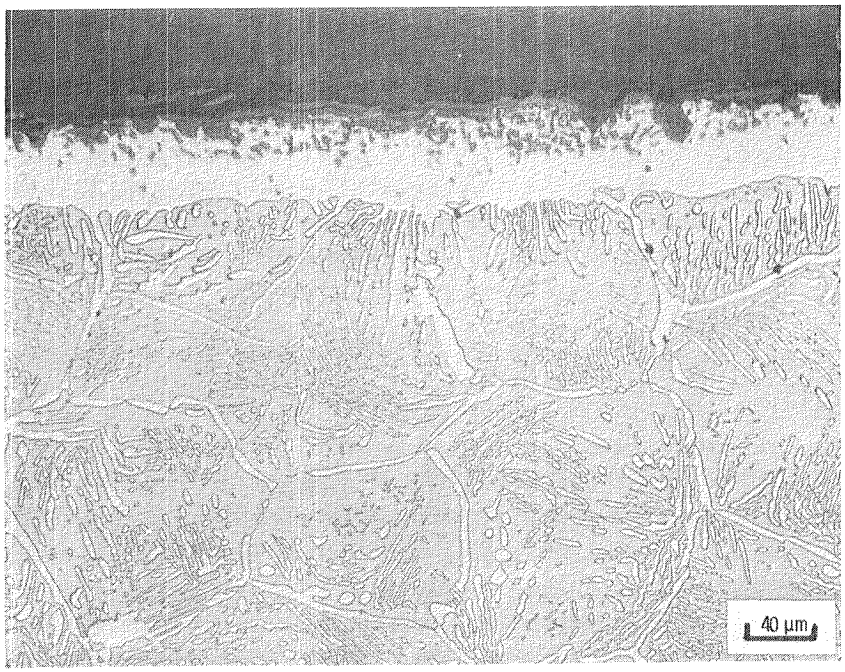

(g) Alloy 16, Co-13.07Cr-24.55Al.

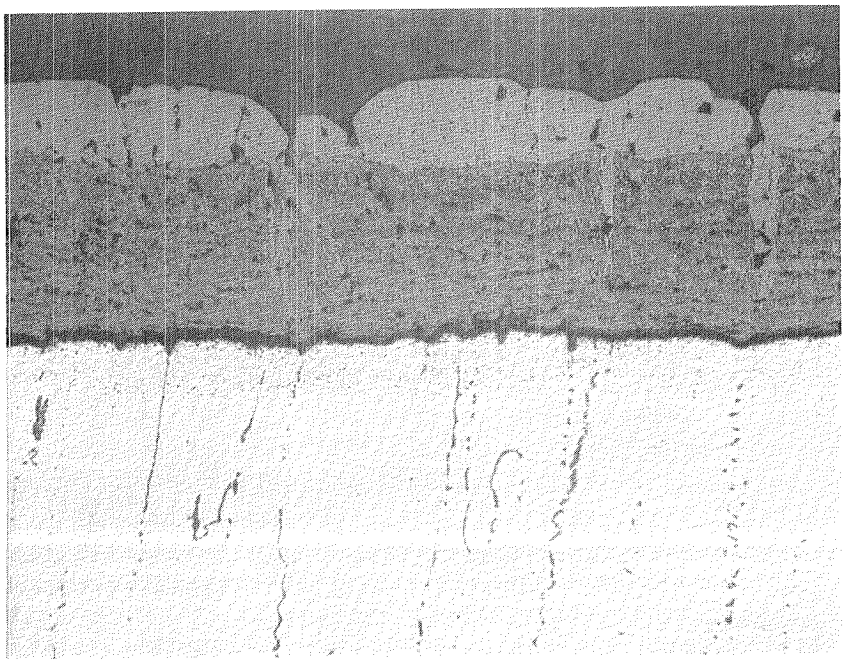

(h) Alloy 17, Co-15.90Cr-5.41Al.

Figure 4. - Continued.

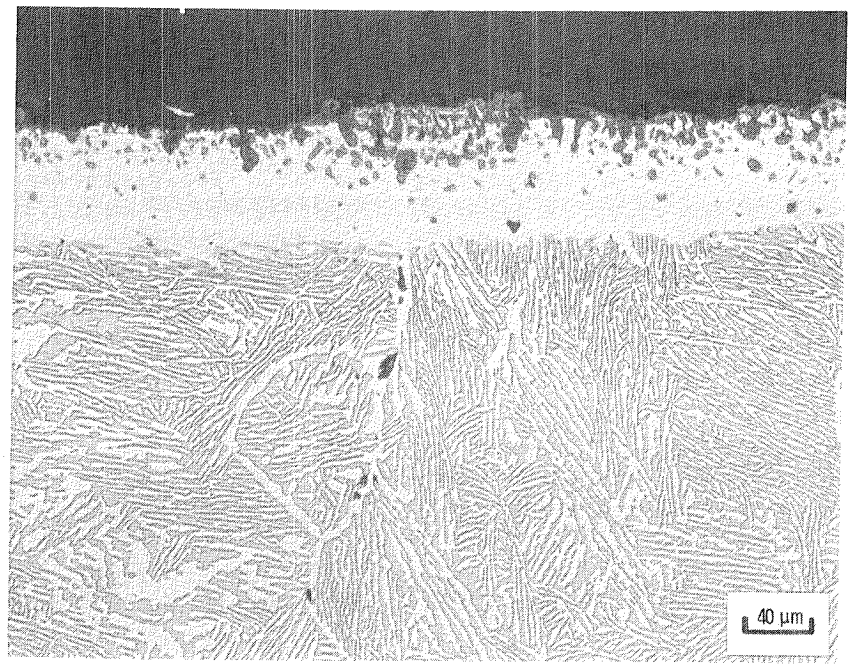

(i) Alloy 18, Co-22.11Cr-16.95Al.

Figure 4. - Concluded.

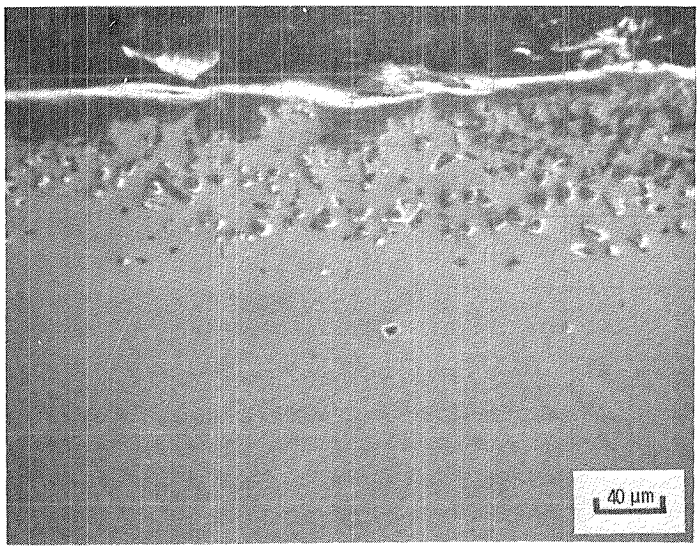

(a) Secondary electron image.

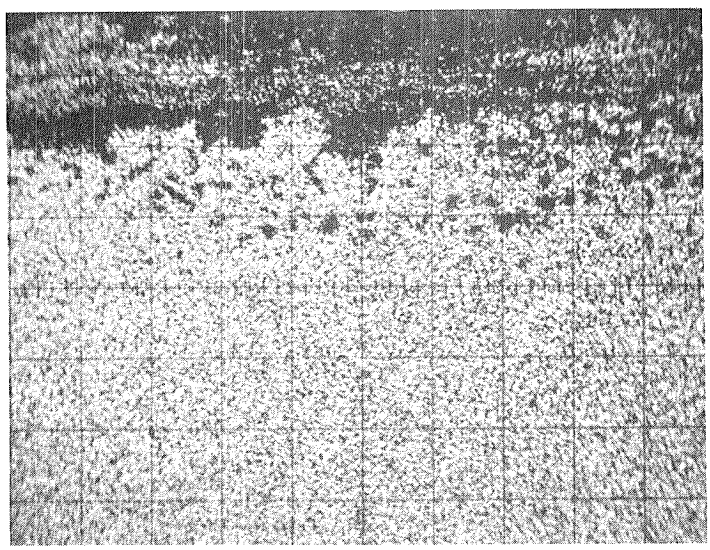

(b) Cobalt Kα.

Figure 5. - Element distribution near surface of alloy 10, Co-15.86Cr-18.30Al. Corroded at 1100° C, 100 cycles. Typical of alloys with a thin retained scale over a depleted zone.

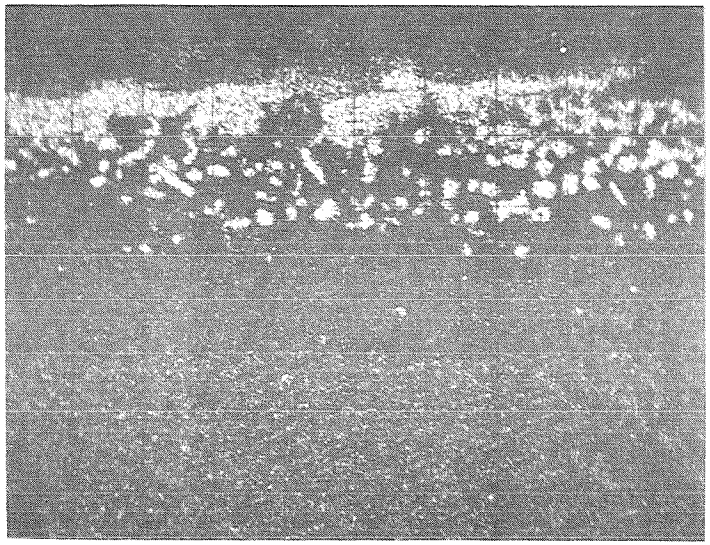

(c) Aluminum Kα.

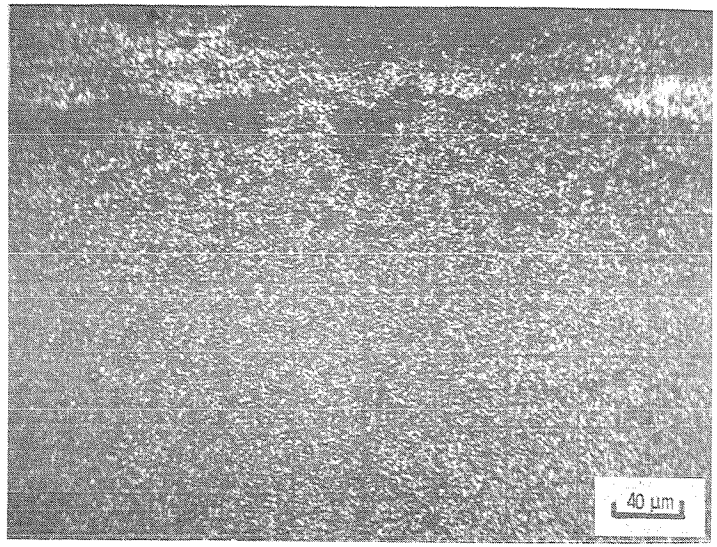

(d) Chromium Kα.

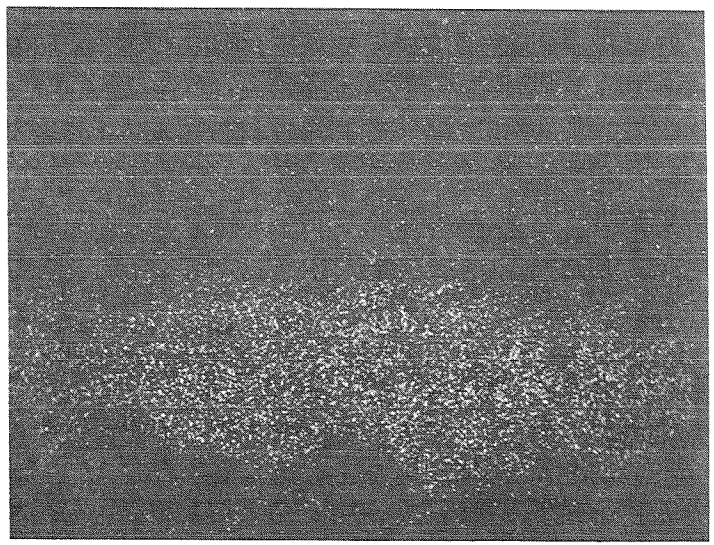

(e) Sulfur Kα.

Figure 5. - Concluded.

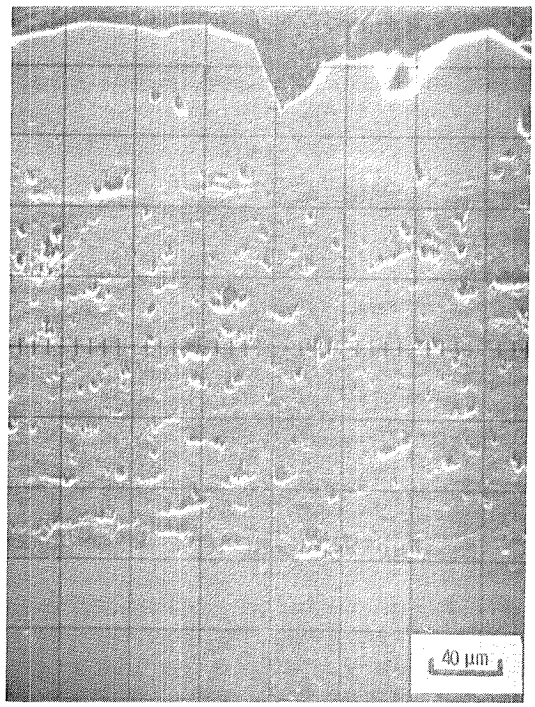

(a) Secondary electron image.

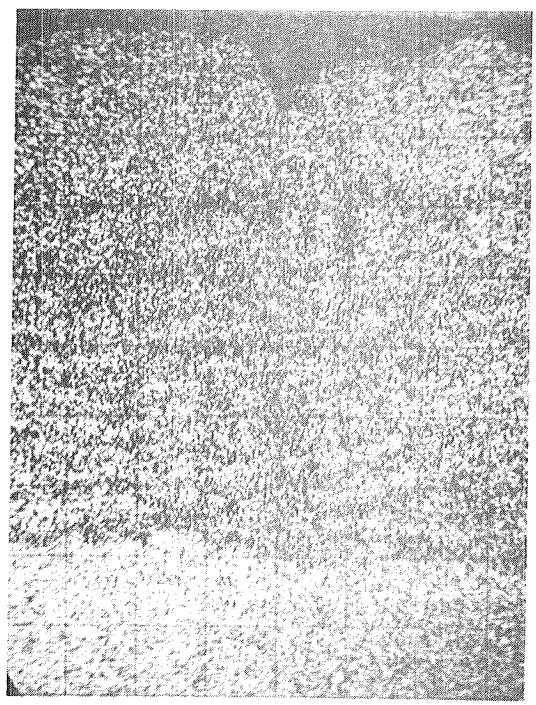

(b) Cobalt Kα.

Figure 6. - Element distribution near surface of alloy 17, Co-15.90Cr-5.41Al. Corroded at 1100° C, 100 cycles. Typical of alloys with double layered scales.

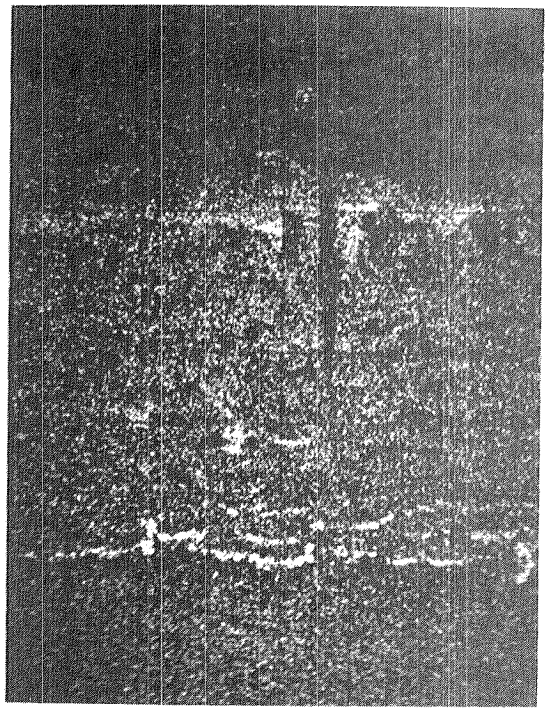

(c) Aluminum Kα.

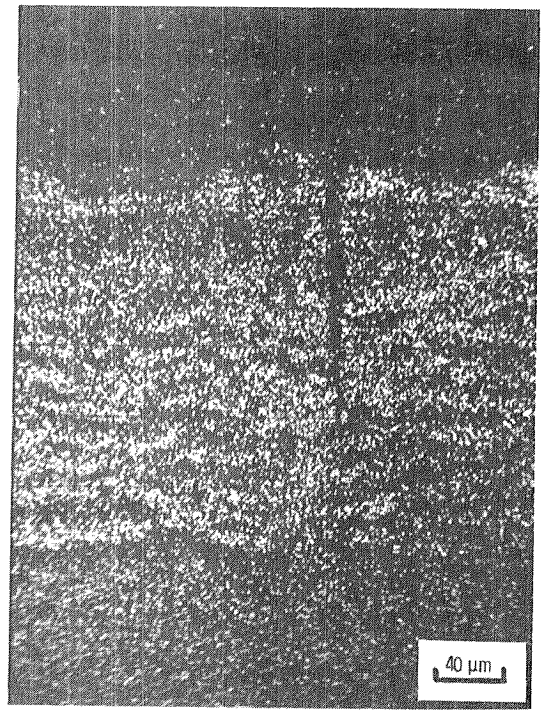

(d) Chromium Kα.

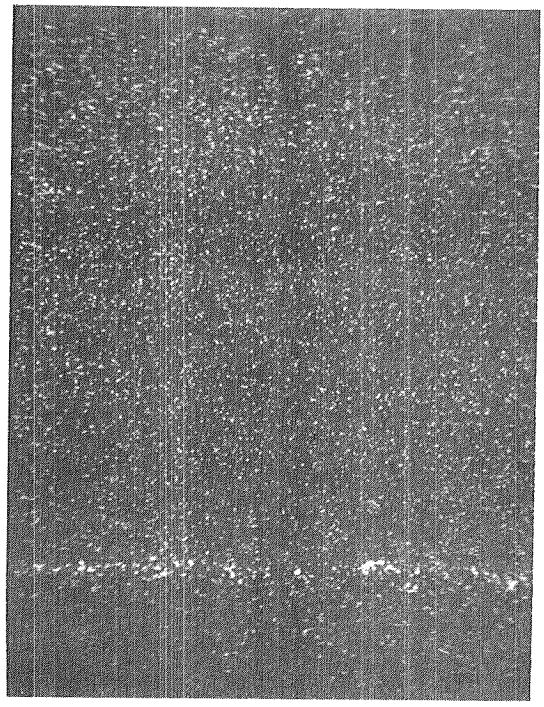

(e) Sulfur Kα.

Figure 6. - Concluded.

	LOG D	D(μm)
C	1.301	20
D	1.699	50
E	2.000	100
F	2.301	200
G	2.699	500

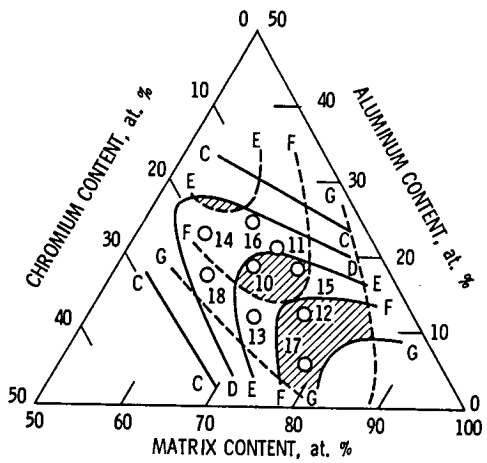

Figure 7. - Corrosion isopleths (logarithm of the maximum depth of attack, D) at 1100° C for CoCrAl alloys (solid contours) and their compositionally equivalent NiCrAl alloys (dash contours). The data point numbers are the designations of the cobalt base alloys. The hash areas are regions where the corrosion of the two alloy systems overlap.

1. Report No. NASA TM-79311	2. Government Accession No.	3. Recipient's Catalog No.
4. Title and Subtitle CORROSION RESISTANCE OF SODIUM SULFATE COATED COBALT-CHROMIUM-ALUMINUM ALLOYS AT 900°, 1000°, AND 1100° C		5. Report Date November 1979 6. Performing Organization Code
7. Author(s) G. J. Santoro		8. Performing Organization Report No. E-267 10. Work Unit No.
9. Performing Organization Name and Address National Aeronautics and Space Administration Lewis Research Center Cleveland, Ohio 44135		11. Contract or Grant No.
12. Sponsoring Agency Name and Address National Aeronautics and Space Administration Washington, D.C. 20546		13. Type of Report and Period Covered Technical Memorandum 14. Sponsoring Agency Code
15. Supplementary Notes		

16. Abstract

A series of cobalt-rich alloys in the cobalt-chromium-aluminum system were coated once with 1 mg/cm^2 of Na_2SO_4 and exposed at temperatures of 900°, 1000°, and 1100° C for 100-one hour cycles. The extent of the corrosion was measured and the results compared to the cyclic oxidation of alloys with the same composition and to the hot corrosion of compositionally equivalent nickel-base alloys. Cobalt alloys with sufficient aluminum content to form aluminum containing scales corroded less than their nickel-base counterparts. The cobalt alloys with lower aluminum levels formed CoO scales and corroded more than their nickel-base counterparts which formed NiO scales.

17. Key Words (Suggested by Author(s))	18. Distribution Statement
Corrosion; Oxidation; Hot corrosion; Cobalt alloys; Cobalt-chromium-aluminum alloys	Unclassified - unlimited STAR Category 26

19. Security Classif. (of this report)	20. Security Classif. (of this page)	21. No. of Pages	22. Price*
Unclassified	Unclassified		

* For sale by the National Technical Information Service, Springfield, Virginia 22161

End of Document